

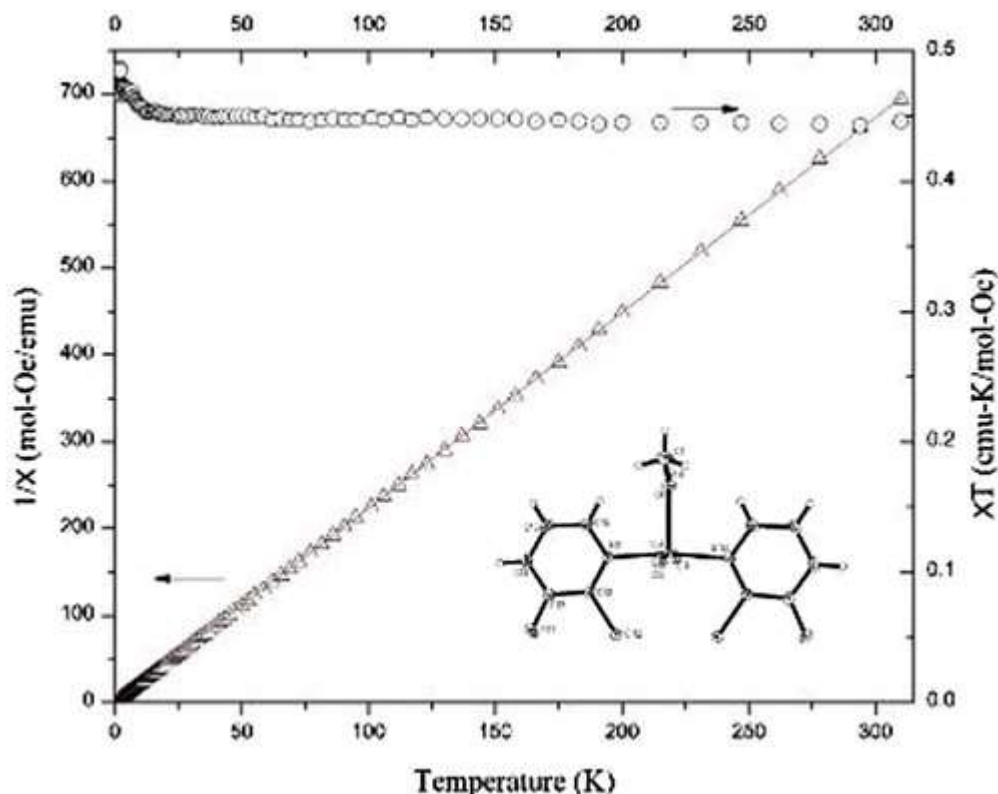
## 2-Chloro-3-fluoropyridine copper (II) complexes and the effect of structural changes on magnetic behavior

Robert J. DuBois,<sup>[a]</sup> Christopher P. Landee,<sup>[b]</sup> Melanie Rademeyer<sup>[c]</sup> and Mark M. Turnbull,<sup>\*,[a]</sup>

[a] Carlson School of Chemistry and Biochemistry and [b] Dept. of Physics, Clark University, 950 Main St., Worcester, Massachusetts 01610 USA

[c] Dept. of Chemistry, University of Pretoria, University of Pretoria, Private bag X20, Hatfield 0028 South Africa

**ABSTRACT:** A family of copper(II) compounds has been prepared with the general formula (2-chloro-3-fluoropyridine)<sub>2</sub>CuX<sub>2</sub>·n(Y) where X = Cl, Br, n=0,1 and Y= methanol or water. For the copper chloride complexes, only solvated structures were obtained (**1**, X = Cl, Y = H<sub>2</sub>O; **2**, X = Cl, Y = CH<sub>3</sub>OH) while for the copper bromide compounds, both a desolvated structure and the methanol solvate were successfully prepared (**3**, X = Br, Y = none; **4**, X = Br, Y = CH<sub>3</sub>OH). Each compound has been characterized by IR, powder X-ray diffraction, single-crystal X-ray diffraction, and temperature dependent magnetic susceptibility measurement. Compounds **1** and **4** are isostructural, in the space group Cm, and neither exhibits significant magnetic exchange although superexchange pathways are present. Compound **2** also crystallizes in the Cm space group and exhibits weak ferromagnetic interactions ( $J/k_B = 1.72(2)$  K from the 1D-ferromagnetic chain model) which are likely propagated by hydrogen bonding. Compound **3** crystallizes in the space group P2<sub>1</sub>/n with the Cu(II) ion sitting on a crystallographic inversion center. Compound **3** exhibits weak antiferromagnetic exchange via two-halide superexchange typical for similar complexes. The magnetic data for **3** were fit to the 1D-antiferromagnetic chain model resulting in  $J/k_B = -1.21(1)$ .



## INTRODUCTION

Coordination chemistry is an ever-expanding field which has received great attention for decades.<sup>1,2,3,4</sup> Within that broad area, copper(II) coordination complexes have been studied for their potential as molecular magnets for decades.<sup>5,6,7</sup> Formation of coordination complexes exhibit a large diversity of geometries and coordination numbers<sup>8,9</sup> and a substantial number of those are displayed by Cu(II) alone.<sup>10</sup> Further, the Cu(II)  $d^9$  system is particularly useful for magnetostructural correlations in such systems as its  $S = \frac{1}{2}$  state makes it a quantum system and one where magnetic superexchange has been observed in a wide variety of crystal lattice types.<sup>11</sup> This broad interest of copper(II) coordination complexes has been accompanied by an increase in use of pyridine<sup>12,13</sup> and substituted pyridine molecules as ligands. Alkyl, amino and halo substituents have been widely used to study correlations between substituents on the pyridine ligand, and its structure and magnetic properties.<sup>14,15,16,17,18,19,20,21,22</sup> We have been interested, for some time, in such structural correlations in copper(II) coordination complexes of the general formula  $L_2CuX_2$  where L is an organic ligand and X is a halide (Cl or Br), especially to examine magnetic exchange through the bihalide and two-halide pathways.<sup>23,24,25,26,27</sup> Some recent studies have focused on families of compounds using 2,3-disubstituted pyridine molecules as ligands, where the substituents were alkyl or halogen groups<sup>28,29</sup> including a system which resulted in an unusual disordered linear chain.<sup>30,31</sup> In these compounds, halogen bonding has been observed, both intra- and intermolecularly, which provides a distinct stabilization of the lattice as well as providing possible magnetic superexchange pathways. Given our prior success in the replacement of methyl substituents on pyridine ligands with halogen atoms,<sup>32,33,34</sup> and the synthesis of a well-described magnetic ladder employing 2,3-dimethylpyridine<sup>35</sup> we became interested in preparing and studying a family of complexes with 2-X-3-X'-pyridine. Here we report the results of our investigations using 2-chloro-3-fluoro-pyridine (2-Cl-3-Fpy) as a ligand including the preparation and characterization of  $(2\text{-Cl-3-Fpy})_2\text{CuCl}_2 \cdot \text{MeOH}$  (**1**),  $(2\text{-Cl-3-Fpy})_2\text{CuCl}_2 \cdot \text{H}_2\text{O}$  (**2**),  $(2\text{-Cl-3-Fpy})_2\text{CuBr}_2$  (**3**) and  $(2\text{-Cl-3-Fpy})_2\text{CuBr}_2 \cdot \text{MeOH}$  (**4**).

## EXPERIMENTAL

2-Chloro-3-fluoropyridine, 1-propanol, acetonitrile and methanol were obtained from Aldrich Chemical Company and used without further purification. Copper chloride dihydrate and copper bromide were purchased from J.T. Baker and used without further purification. IR spectra were recorded via ATR on a Perkin-Elmer Spectrum 100 IR spectrophotometer. X-Ray powder diffraction data were collected on a Bruker AXS-D8 X-ray Powder Diffractometer. Elemental analyses were determined by Marine Science Institute, University of California, Santa Barbara CA 93106.

### **Bis(2-chloro-3-fluoro-pyridine)dichlorocopper(II)·methanol (1).**

Liquid 2-chloro-3-fluoro-pyridine (0.132g, 1.0 mmol) was added dropwise to a solution of copper(II) chloride dihydrate (0.088g, 0.52 mmol) in 5.0 ml of methanol. A light green solution resulted and no precipitate formed. The beaker was covered in Parafilm with a few small holes in the film and the solution was allowed to evaporate at room temperature. After seven days of slow evaporation a large amount of dark blue, square crystals were present in solution. The mixture was suction filtered and the dark blue crystals washed with cold methanol and allowed to dry to yield 0.139 g (69.8%). No attempt was made to maximize yield. IR( $\nu$ ,  $\text{cm}^{-1}$ ): 3414b, 3099w, 3055 m, 2941w, 2835w, 1594m, 1573m, 1447w, 1429s, 1356w, 1273m, 1218m, 1109m, 1004s, 946m, 856w, 809s, 721s, 700 s. CHN for  $\text{C}_{11}\text{H}_{10}\text{N}_2\text{OF}_2\text{Cl}_4\text{Cu}$ , found (calc.) C: 30.35 (30.76), H: 2.27 (2.35), N: 6.31(6.52).

### **Bis(2-chloro-3-fluoro-pyridine)dichlorocopper(II)·H<sub>2</sub>O (2).**

Liquid 2-chloro-3-fluoropyridine (0.263 g, 2.0 mmol) was added dropwise to a solution of copper(II) chloride dihydrate (0.171 g, 1.0 mmol) in 1.0 ml of 1-propanol . A light green solution resulted and no precipitate formed. The beaker was covered in Parafilm with a few small holes in the film and the solution was allowed to evaporate at room temperature.. After one day, a large amount of flat turquoise crystals were visible. The mixture was suctioned filtered, and the turquoise crystals washed with cold methanol and allowed to dry to give 0.130 g (31.3%). No effort was made to maximize yield. IR ( $\nu$ ,  $\text{cm}^{-1}$ ): 3578b, 3105s, 3048s, 1595m, 1572m, 1450w, 1427s, 1274m, 1248m, 1220m, 1203m, 1136m, 1110s, 991m, 953m, 812s, 722s, 702s. CHN for  $\text{C}_{10}\text{H}_8\text{N}_2\text{OF}_2\text{Cl}_4\text{Cu}$ , found (calc.) C: 28.53 (28.90), H: 2.03 (1.94), N: 6.38 (6.74).

### **Bis(2-chloro-3-fluoro-pyridine)dibromocopper(II) (3).**

Copper(II) bromide (0.167g,0.75 mmol) was dissolved in 20.0 ml of 1-propanol via a heated stir plate. Liquid 2-chloro-3-fluoropyridine (0.195g, 1.48 mmol) was then added to the copper(II) bromide solution dropwise. A red solution resulted with no formation of precipitate. The solution was then covered with a piece of filter paper and allowed to evaporate slowly. After 19 days, a mass of black thin rectangular crystals were present in ~5.0 ml of solution. The mixture was suctioned filtered and the black crystals washed with cold 1-propanol and allowed to dry to give 0.087 g (23.9 % yield). After four days, a large mass of black crystals were recovered from the filtrate (0.075g , 20.6 % ). Overall yield 44.5% yield (0.162 g). No effort was made to maximize yield. IR( $\nu$ ,  $\text{cm}^{-1}$ ): 3095w, 3055w, 1599w, 1578m, 1450w, 1430s, 1408m, 1269m, 1214m, 1167w, 1118m, 1077w, 1057w, 865w, 803s, 717m, 706m. CHN for  $\text{C}_{10}\text{H}_6\text{N}_2\text{OF}_2\text{Cl}_2\text{Br}_2\text{Cu}$ : found (calc.) C: 24.29 (24.67), H: 1.32 (1.24), N:5.57 (5.76).

#### **Bis(2-chloro-3-fluoropyridine)dibromocopper(II)·methanol (4).**

Copper(II) bromide (0.116 g, 0.52 mmol) was dissolved in 5.0 ml of methanol in a 10.0 ml beaker on a heated stir plate. This resulted in a dark red colored solution to which liquid 2-chloro-3-fluoropyridine (0.132 g, 1.0 mmol) was added dropwise. No precipitate formed and solution was covered with a piece filter paper and left on the desktop to slowly evaporate. One day later a mass of black crystals were present in a minimal volume of solution. The mixture was suctioned filtered and the black crystals washed with cold 1-propanol. (0.159g, 61.3 %). No further effort was made to maximize yield. IR ( $\nu$ ,  $\text{cm}^{-1}$ ): 3408b, 3101w, 3049w, 1594m, 1573m, 1446w, 1428s, 1351w, 1273m, 1244w, 1216m, 1135m, 1110s, 1001s, 944w, 856w, 808s, 720m, 701s. CHN for  $\text{C}_{11}\text{H}_{10}\text{N}_2\text{O}\text{F}_2\text{Cl}_2\text{Br}_2\text{Cu}$ : found (calc. ) C: 25.28 (25.48), H: 1.52 (1.94), N: 5.74(5.40).

#### **Magnetic data**

Magnetic data for compounds **1-4** were collected using a Quantum Design MPMP-XL SQUID magnetometer. Crystalline samples were powdered and mounted in a gelatin capsule which was then placed in a plastic straw. Magnetization was measured as a function of applied field from 0 – 50 kOe; several data points were recollected as the field was returned to zero to check for hysteresis effects; none were seen. All plots were linear to at least 5 kOe. Magnetic susceptibility was then measured between 1.8 and 310 K in an applied field of 1 kOe. Data were corrected for the background of the gelatin capsule and straw (measured independently), for the temperature independent paramagnetism of the copper(II) ion ( $60 \times 10^{-6}$  emu/mol·Oe) and for the diamagnetic contributions of the constituent atoms, as estimated from Pascal's constants.<sup>36</sup> Powder X-ray diffraction data was collected on the samples used for magnetic data collection to check for impurities and verify that the samples were the same phase as the single crystals.

#### **Single-crystal X-ray diffraction data**

Data collections were carried out on a Bruker D8 Venture diffractometer equipped with a Photon 100 CMOS detector employing graphite-monochromated Mo-K $\alpha$  radiation, using  $\varphi$  and  $\omega$  scans. Using the SAINT+ software,<sup>37</sup> the data was reduced and absorption corrections were made using the SADABS program.<sup>38</sup> The structures were solved using SHELXS-97<sup>39</sup> and refinement was carried out via least squares analysis using SHELXL-2014.<sup>40</sup> Non-hydrogen atoms were refined using anisotropic thermal parameters. Hydrogen atoms bonded to carbon were placed in calculated positions and refined using isotropic thermal parameters and a riding model. Hydrogen atoms bonded to oxygen were located in the difference Fourier maps and their positions refined with fixed isotropic thermal parameters.

Crystallographic information for compounds **1-4** can be found in Table 1. Structural data for compounds

**1-4** can be seen in Tables 2-4. The structures have been deposited with the CCDC as deposit numbers 1851561, **2**; 1851562, **4**, 1851563, **2RT**; 1851564, **1**; 1851565, **3**.

**Table 1:** Crystal and experimental data for **1-4**.

	<b>1</b>	<b>2RT</b>	<b>2</b>	<b>3</b>	<b>4</b>
Formula	C <sub>11</sub> H <sub>10</sub> N <sub>2</sub> OF <sub>2</sub> Cl <sub>4</sub> Cu	C <sub>10</sub> H <sub>8</sub> N <sub>2</sub> OF <sub>2</sub> Cl <sub>4</sub> Cu	C <sub>10</sub> H <sub>8</sub> N <sub>2</sub> OF <sub>2</sub> Cl <sub>4</sub> Cu	C <sub>10</sub> H <sub>6</sub> N <sub>2</sub> F <sub>2</sub> Cl <sub>2</sub> Br <sub>2</sub> Cu	C <sub>11</sub> H <sub>10</sub> N <sub>2</sub> OF <sub>2</sub> Cl <sub>2</sub> Br <sub>2</sub> Cu
Mol. Wt. (g/mol)	413.51	415.52	415.52	486.43	518.47
T(K)	150(2)	298(2)	150(2)	150(2)	150(2)
Wavelength(Å)	0.71073	0.71073	0.71073	0.71073	0.71073
Crystal system	Monoclinic	Monoclinic	Monoclinic	Monoclinic	Monoclinic
Space group	Cm	Cm	Cm	P2 <sub>1</sub> /n	Cm
a (Å)	7.6637(7)	7.1137(9)	6.9886(4)	6.3820(4)	7.8944(5)
b (Å)	15.4397(14)	15.6491(17)	15.6147(7)	17.3224(12)	15.7063(9)
c (Å)	6.4475(6)	6.3834(8)	6.3455(3)	6.9201(5)	6.6381(4)
β(°)	98.656(4)	94.126(4)	93.731(2)	114.323(2)	101.405(2)
V (Å <sup>3</sup> )	754.21(12)	708.78(15)	690.98(6)	697.12(8)	806.82(8)
Z	2	2	2	2	2
Crystal size(mm)	0.318x0.214x0.124	0.411x0.334x0.185	0.154x0.143x0.069	0.593x0.392x0.220	0.462x0.375x0.240
Abs. co. (mm <sup>-1</sup> )	2.171	2.310	2.370	7.688	6.654
F(0,0,0)	406	410	410	462	498
Θ <sub>range</sub> (°)	2.64 to 32.00	2.60 to 30.70	2.609 to 28.399	2.35 to 28.77	2.594 to 28.427
Index ranges	-11 ≤ h ≤ 11 -22 ≤ k ≤ 22 -9 ≤ l ≤ 9	-10 ≤ h ≤ 10 -22 ≤ k ≤ 22 -9 ≤ l ≤ 9	-9 ≤ h ≤ 9 -20 ≤ k ≤ 20 -8 ≤ l ≤ 8	-8 ≤ h ≤ 8 -23 ≤ k ≤ 23 -9 ≤ l ≤ 9	-10 ≤ h ≤ 10 -20 ≤ k ≤ 20 -8 ≤ l ≤ 8
Rfln. Coll.	17058	15354	11351	36415	12451
Flack parameter	0.056(7)	0.0556	0.040(4)		0.271(15)
Ind. rfln (R <sub>int</sub> )	2698 (0.0450)	2267(0.0513)	1800(0.0300)	1813 (0.1393)	2090(0.0573)
Data/Restraints/ parameters	2698 / 5 / 110	2267/3/102	1800/2/101	1813/0/88	2090/4/112
Final R (R1)	0.0308	0.0233	0.0164	0.0363	0.0269
[I>2σ(I)] (wR2)	0.0627	0.0505	0.0393	0.0641	0.0597
R index (R1)	0.0379	0.0272	0.0175	0.0534	0.0344
(all data) (wR2)	0.0652	0.0518	0.0394	0.0680	0.0624
Final peak/hole (e/Å <sup>3</sup> )	0.855 and -0.850	0.347 and -0.441	0.224 and -0.364	0.704 and -0.970	0.515 and -0.556

**Table 2:** Bond Lengths (Å) and angles (°) for **1-4**

<u>Bond Lengths</u>	<b>1</b>	<b>2RT</b>	<b>2</b>	<b>3</b>	<b>4</b>
Cu1-X1	2.2429(13)	2.2648(11)	2.2751(11)	2.3884(4)	2.4046(15)
Cu2-X2	2.2567(13)	2.2696(11)	2.2796(10)	-	2.3866(14)
Cu1-N11	2.064(2)	2.0536(19)	2.0495(19)	1.993(3)	2.046(4)
Cu1-O1	2.309(3)	2.397(3)	2.337(3)	-	2.301(6)
O1-H1(A)	0.78(7)	0.84(3)	0.83(3)	-	0.86(11)
O1-H1B	-	0.83(3)	0.84(3)	-	-
<u>Bond Angles</u>					
X1-Cu-X2	170.97(4)	173.15(4)	171.68(4)	180.0	171.45(5)
X1-Cu-N11	88.94(10)	90.07(8)	89.99(8)	90.33(8)	88.7(2)
X2-Cu-N11	90.44(10)	89.55(8)	89.53(8)	89.67(8)	90.7(2)
N11-Cu-N11	171.99(16)	173.55(15)	173.30(14)	180.00(12)	172.5(3)
X1-Cu-O1	94.25(9)	101.09(9)	101.70(8)	-	93.76(15)
X2-Cu-O1	94.78(9)	85.76(9)	93.28(7)	-	94.79(15)
N11-Cu-O1	93.93(8)	93.15(7)	93.28(7)	-	93.60(15)

**Table 3:** Hydrogen bonding for compounds **1-4**

<u>Compound</u>	<u>D-H...A</u>	<u>d(D-H)</u>	<u>D(H...A)</u>	<u>d(D...A)</u>	<u>&lt;(DHA)</u>
<b>1</b>	O1-H1...Cl2A	0.78(7)	2.42(7)	3.136(4)	152(6)
<b>2RT</b>	O1-H1B...Cl1B	0.84(3)	2.87(5)	3.700(4)	176(6)
	O1-H1A...Cl2A	0.84(3)	2.37(3)	3.213(3)	177(6)
<b>2</b>	O1-H1B...Cl1C	0.84(3)	2.74(3)	3.572(3)	177.4
	O1-H1A...Cl2D	0.83(3)	2.36(3)	3.186(3)	173(5)
<b>4</b>	O1-H1...Br1D	0.86(11)	2.45(11)	3.244(6)	154(8)

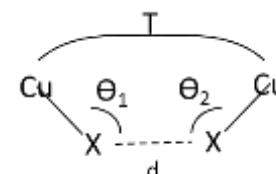
Symm. Op.: A (x,y,z-1), B (x-1,y,z), C (x+1,y,z), D (x,y,z+1)

**Table 4:** Halogen bonding parameters in **1-4**

	<b>1</b>	<b>2RT</b>	<b>2</b>	<b>3</b>	<b>4</b>
C12-Cl12...X1-Cu1	3.376	3.326	3.290	3.442	3.477
C-X...X	164.0	168.9	169.3	172.9	161.9
X...X-Cu	107.1	104.4	103.6	99.4	108.8

**Table 5:** Comparison of two-halide superexchange pathway parameters of **1-4**

	<b>1</b>	<b>2RT</b>	<b>2</b>	<b>3</b>	<b>4</b>
d (Å)	4.234	3.990	3.938	4.395	4.177
$\Theta_1$ (°)	127.5	109.7	114.9	103.9	127.8
$\Theta_2$ (°)	118.5	116.6	106.6	103.9	119.3
T(°)	180	180	180	180	180



## RESULTS

### Syntheses

Reaction of 2-Cl-3-Fpy with  $\text{CuX}_2 \cdot n\text{H}_2\text{O}$  (X = Cl, Br; n = 0,2) resulted in the formation of a family of compounds with the general formula  $[(2\text{-Cl-3-Fpy})_2\text{CuX}_2(\text{sol})_x]$  where there may be a solvent molecule (water, methanol) coordinated to the Cu ion. The complexes  $(2\text{-Cl-3-Fpy})_2\text{CuCl}_2 \cdot \text{MeOH}$  (**1**),  $(2\text{-Cl-3-Fpy})_2\text{CuCl}_2 \cdot \text{H}_2\text{O}$  (**2**),  $(2\text{-Cl-3-Fpy})_2\text{CuBr}_2$  (**3**) and  $(2\text{-Cl-3-Fpy})_2\text{CuBr}_2 \cdot \text{MeOH}$  (**4**) were isolated and single crystal structures of **1-4** were obtained. Repeated efforts to crystallize the non-solvated form of  $(2\text{-Cl-3-Fpy})_2\text{CuCl}_2$  were unsuccessful regardless of the solvents employed. Either solvated material, including incorporation of serendipitous moisture from the air, or powders were obtained. Attempts were made to produce the non-solvated material through gentle heating of both **1** and **2**. As shown by both a color change (from blue to light green) and IR, it was indeed possible to remove the solvent, but the ligand was sufficiently volatile so that portions of the ligand were lost as well. If the resulting powder was allowed

to sit in air, it absorbed water and converted to a hydrated form, as confirmed by the color change back to blue and by IR, but powder X-ray diffraction indicated that the new material was a mixture of **2** and an unknown compound.

## Crystal Structures

### Bis(2-chloro-3-fluoropyridine)dichlorocopper(II)·methanol (**1**).

Compound **1** crystallizes in the monoclinic space group Cm. The molecular unit is shown in Figure 1. Selected bond lengths and angles are given in Table 2. The Cu(II) ion and two chloride ions are located on a crystallographic mirror with one 2-Cl-3-Fpy ligand in a general position. The methanol molecule sits athwart the mirror. The Cu(II) is thus five-coordinate with an Addison parameter ( $\tau$ )<sup>41</sup> of 0.017, indicating that the Cu(II) ion is nearly square pyramidal; Cu1 lies 0.128 Å above the mean basal plane. The apical methanol molecule is almost perfectly perpendicular with an angle of 0.02° between the Cu1-O1 bond and the normal to the basal plane. Similarly, the pyridine rings, which are nearly planar (mean deviation of 0.0021 Å of the constituent atoms) are close to perpendicular to the basal plane at a canting angle of 82.2°. The pyridine rings are inclined 7.1° to each other with both tipped slightly toward Cl2. The molecule is in the syn-conformation with the substituents on the pyridine rings directed toward the same face of the basal plane.

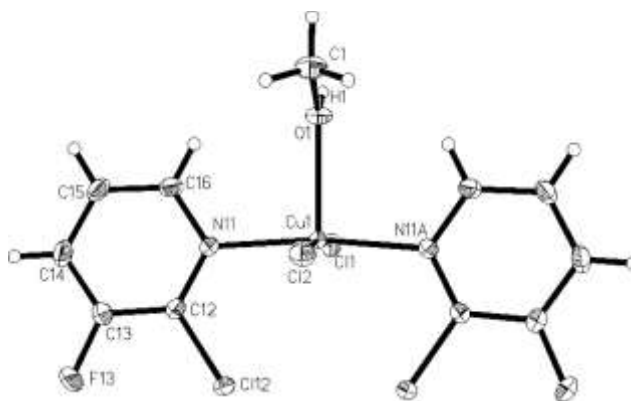


**Figure 1:** A plot of the molecular unit of compound **1** showing 50% probability thermal ellipsoids. The asymmetric unit, copper coordination sphere and hydrogen atom whose position was refined are labeled.

Molecules of **1** are linked into chains parallel to the *c*-axis by hydrogen and halogen bonds (Figure 2a). The O1...Cl2 hydrogen bond ( $d_{\text{Cl2}\dots\text{O1A}} = 3.136(4)$  Å) complements symmetry equivalent pairs of Cl2...Cl1 halogen bonds, connecting the same pairs of molecules (details of hydrogen and halogen bonds are found in Tables 3 and 4, respectively).

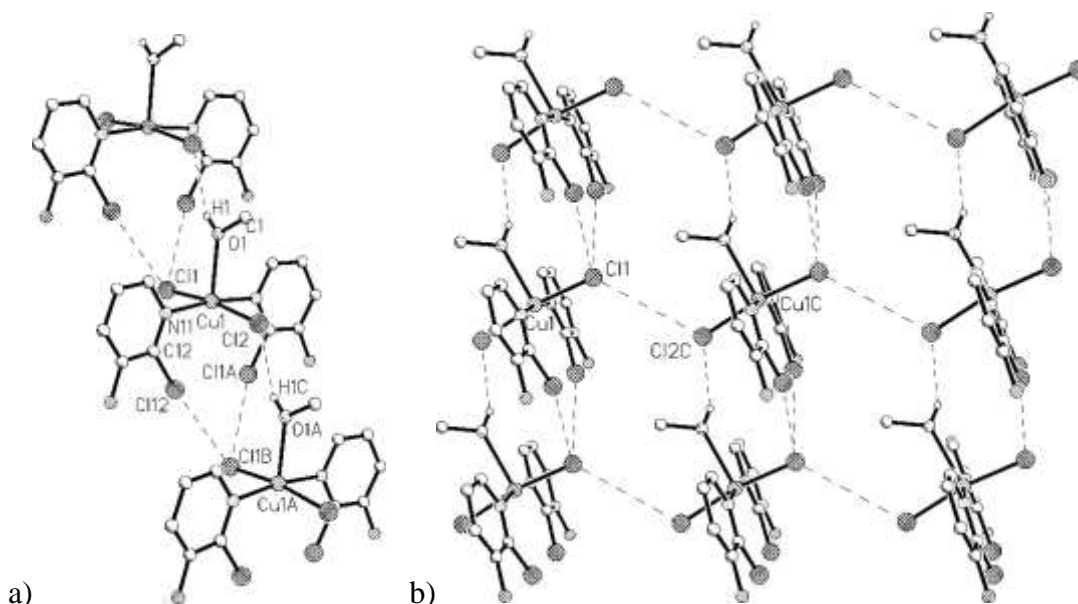


**Figure 2.** a) A plot of the chain structure of **1**. b) A plot of the layer structure of **1**. Dashed lines represent hydrogen and halogen bonds and short chloride...chloride contacts. Hydrogen atoms not involved in hydrogen bonds have been omitted for clarity.

The chlorine-chloride halogen bond is typical Type 1, with a Cl12...Cl1B distance of 3.376 Å and bond angles near 180° and 90°. The chains are further linked into layers via chloride...chloride contacts parallel to the *a*-axis ( $d_{\text{Cl11}\dots\text{Cl2c}} = 4.23\text{Å}$ ). Although the latter contacts are well outside the sum of the van de Waals radii, this two-halide pathway has been shown to propagate magnetic exchange at distances greater than 4.5 Å.<sup>33</sup> The layers are stacked parallel to the *b*-axis with the pyridine rings interdigitated (Figure 3). However, there are no significant  $\pi$ -stacking interactions; the rings are not parallel (by 7.1°), the distance between the ring centroids is greater than 3.9 Å and the slip angle averages 23.5°. The closest halogen...halogen separations between interdigitated rings are between chlorine and fluorine atoms (3.92Å), but both the C-X...X angles are near 90°, which does not support the presence of halogen bonds.



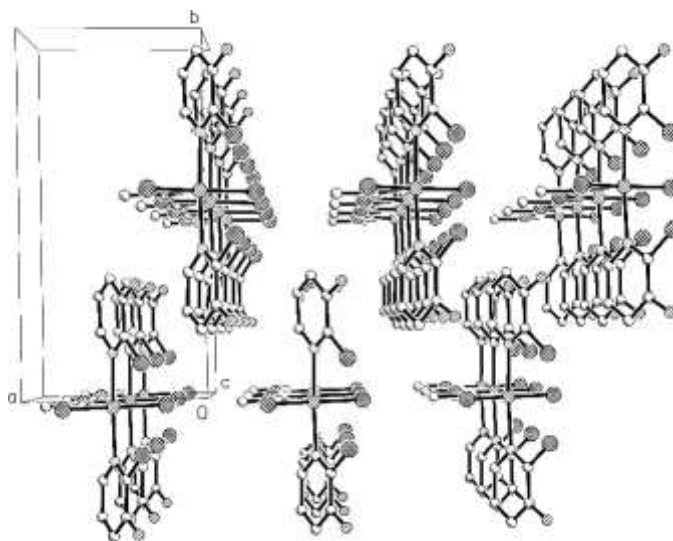


**Figure 3:** Packing diagram showing the interdigitation of the pyridine rings parallel to the *b*-axis. Hydrogen atoms have been removed for clarity.

### **Bis(2-chloro-3-fluoro-pyridine)dichlorocopper(II)·H<sub>2</sub>O (2).**

Compound **2** also crystallizes in the monoclinic space group *Cm*. The molecular unit is shown in Figure 4. Selected bond lengths and angles are given in Table 2. The asymmetric unit is comparable to that of **1** with the coordinated methanol molecule replaced by a water molecule. A very similar structure has been observed previously with 2-methylpyridine,<sup>21</sup> or 2-chloropyridine as the nitrogenous ligand.<sup>42</sup> The coordination sphere about the central Cu(II) ion is again square pyramidal with  $\tau = 0.027$ . The Cu(II) ion lies 0.1138 Å above the basal coordination plane, slightly less than in **1**. The pyridine rings are again planar (mean deviation = 0.0056 Å), but they are canted slightly more away from the normal (78.4°) and again show a syn-conformation for the ring substituents. The greatest difference in the molecular structure of **2**, compared to **1**, is the distinct tilt of the Cu1-O1 bond which is inclined 7.5° from the normal to the basal plane, most likely due to hydrogen bonding (*vide infra*).

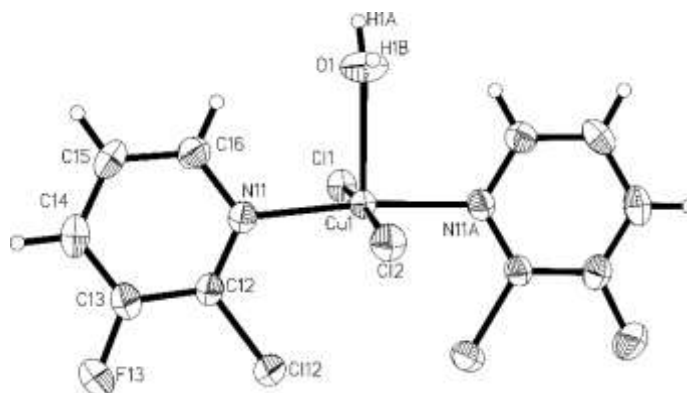


**Figure 4:** A plot of the molecular unit of compound **1** showing 50% probability thermal ellipsoids. The asymmetric unit, copper coordination sphere and hydrogen atom whose position was refined are labeled.

As previously observed, the molecular units are linked into chains parallel to the *c*-axis via a combination of hydrogen ( $d_{O1...Cl2A} = 3.186(3)\text{\AA}$ ) and halogen ( $d_{Cl1...Cl1C} = 3.290\text{\AA}$ ) bonds (full bonding details are found in Tables 3 and 4 respectively) (Figure 5). Although the hydrogen bond appears to be slightly weaker, based on the D...A distance, the halogen bond is clearly stronger, with a shorter halogen...halide distance and angles closer to  $180^\circ$  and  $90^\circ$  respectively.

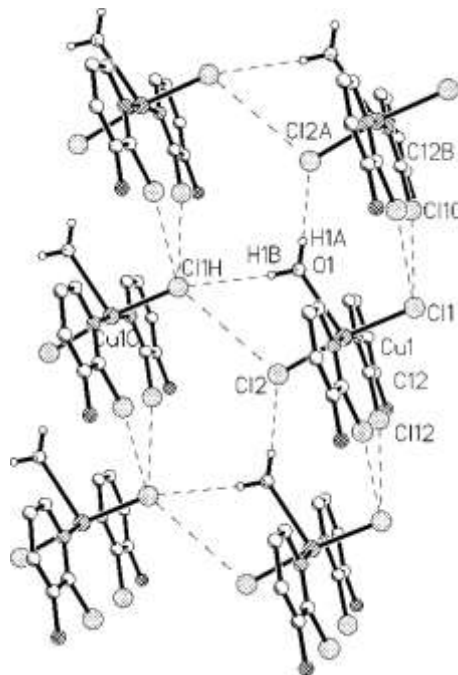


**Figure 5.** A plot showing the formation of chains parallel to the *c*-axis (vertical) via hydrogen and halogen bonds (dashed lines) and the linking of those chains parallel to the *c*-axis (horizontal) via hydrogen bonds and short halide...halide contacts.

The chains are again linked into layers via short chloride...chloride contacts parallel to the *a*-axis ( $d_{Cl2...Cl1H} = 3.938\text{\AA}$ ) while the conversion of the methyl group in **1** to a hydrogen atom in **2** allows for the formation of an additional, weak hydrogen bond ( $d_{O1...Cl1H} = 3.572(3)\text{\AA}$ ) further stabilizing the interchain interactions. Adjacent layers have their pyridine rings interdigitated, as in **1** (Figure 3), but in **2** the possibility of  $\pi$ -stacking interactions is much more likely. Adjacent rings are closer to parallel (canted  $3.4^\circ$ ), the distance between adjacent ring centroids is significantly shorter ( $3.662\text{\AA}$ ) and the slip angle is comparable ( $25.2^\circ$ ). The proximity of the rings again results in short halogen...halogen distances, but the C-X...X angles are near  $90^\circ$  and thus there is unlikely to be any halogen bonding.

With the increased interactions between chains due to the additional hydrogen bond, we were interested in how great an effect temperature would have on the inter chain interactions since the two-halide pathway was the most likely magnetic superexchange pathway, and thus we undertook a room temperature crystal structure study of **2**. Data collection parameters, bond lengths, angles ... are

provided in the tables as **2RT**. As expected, there were some differences in the structures primarily due to the expected thermal expansion. Hydrogen and halogen bonds have lengthened slightly as have the chloride...chloride contact distances. Perhaps surprisingly, however, the complex appears to be even closer to square pyramidal with  $\tau = 0.007$  and the Cu(II) ion lying only 0.100 Å above the basal coordination plane. The Cu1-O1 bond is comparably inclined ( $7.7^\circ$ ) from the normal to the basal plane.

### **Bis (2-chloro-3-fluoro-pyridine)dibromocopper(II)(3).**

Compound **3** crystallizes in the monoclinic space group  $P2_1/n$ . The molecular unit is shown in Figure 6. The Cu(II) ion sits on a crystallographic inversion center and thus the asymmetric unit comprises one 2-Cl-3-Fpy ligand, one bromide ion and one-half Cu(II) ion. The coordination sphere about the copper(II) ion is nearly square planar with a N11-Cu1-Br1 angle of  $89.67(8)^\circ$ ; Cu1, Br1, Br1A, N11 and N11A are coplanar as required by symmetry. Bond lengths and angles within the pyridine ring are comparable to those of related structures (Compounds **1** and **2**). As typical, the pyridine rings are nearly planar (mean deviation = 0.0056 Å) and rotated  $86.1^\circ$  relative to the copper coordination plane in an anti-conformation.

It is common for anti-conformation pyridine rings to form bihalide bridged chains,<sup>27,43</sup> but it is equally common for such formation to be inhibited due to steric strain<sup>18,22,44</sup> as is observed in this case; the closest Br...Cu contact between molecular units is greater than 5.5 Å. Two other interactions occur, however, which generate chain structures. Pairs of halogen bonds form linking the molecules parallel to the *c*-axis ( $d_{\text{Br1}\dots\text{Cl1b}} = 3.442$  Å, Figure 7a), while short Br...Br contacts (4.395 Å, Figure 7b) link the molecules parallel to the *bc*-face diagonal (details of halogen bonds and two halide pathway contacts are found in Tables 4 and 5, respectively).

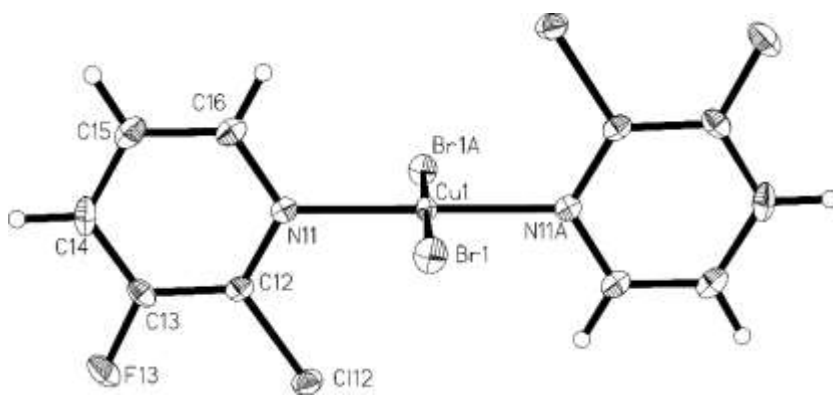


**Figure 6:** A plot of the molecular unit of compound **3** showing 50% probability thermal ellipsoids. The asymmetric unit and copper coordination sphere are labeled. All hydrogen atoms were placed geometrically.

The two-halide pathway connections are further stabilized by interactions between the bromide ions and the adjacent pyridine ring. Br1 lies only 3.424 Å from C13C (Figure 7b) with a Cu1-Br1...C13C angle of 171.4°. In addition, the C13C...Br1 vector is tilted only 4.5° from the normal to the pyridine ring.

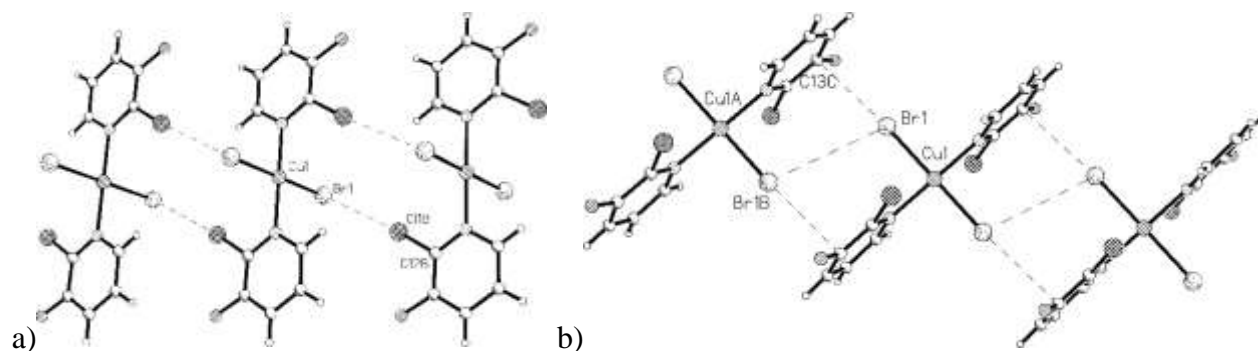


**Figure 7:** A plot of the packing of compound **3** showing a) halogen-bonded chains and b) two-halide pathway chains. Dashed lines represent halogen bonds and short Br...Br and Br...C contacts.

There are close contacts present in the lattice which do not contribute towards magnetic exchange. These contacts occur between chlorine substituents on the pyridine ring and bromide ions with a C11...Br1 distance of 3.442 Å. Close contacts between chlorine substituents on the pyridine ring and fluorine substituents on the pyridine ring of the nearest neighbor molecular unit of **3** are also present with a C11...F1 distance of 3.360 Å. These contact distances are within the sum of the van der Waals radii of the two atoms (vdW radius Br, 1.85 Å; Cl, 1.75 Å). Close contacts such as these, between halide ions and halogen atoms, have been reported in the literature and it is believed that crystal packing is influenced by such interactions.<sup>45</sup>

#### **Bis(2-chloro-3-fluoro-pyridine)dibromocopper(II)·methanol (4).**

Compound **4** crystallizes in the monoclinic space group *Cm* and is isostructural with the chloride analogue, **1**; thus it will be discussed only briefly. The molecular unit is shown in Figure 8 and selected bond lengths and angles are presented in Table 2. The Addison parameter ( $\tau$ ) for the Cu(II) ion is 0.017, identical to that for **1**, again indicating that the Cu(II) ion has a near square pyramidal geometry; the Cu(II) ion lies 0.123 Å above the mean basal plane which shows a mean deviation of the constituent atoms of 0.0492 Å. The oxygen atom of the methanol molecule is only slightly more inclined relative to the basal plane (0.5° from the normal). Similarly, the pyridine rings are virtually planar and close to perpendicular to the basal plane (canting angle = 82.8°) and comparably tipped (7.9°) relative to each other in the syn-conformation. Halogen and hydrogen bonding are observed as before (see Tables 3 and

4), linking the molecules into chains, while short Br...Br contacts, nearly identical to **1**, link the chains into layers (see Figure 2).

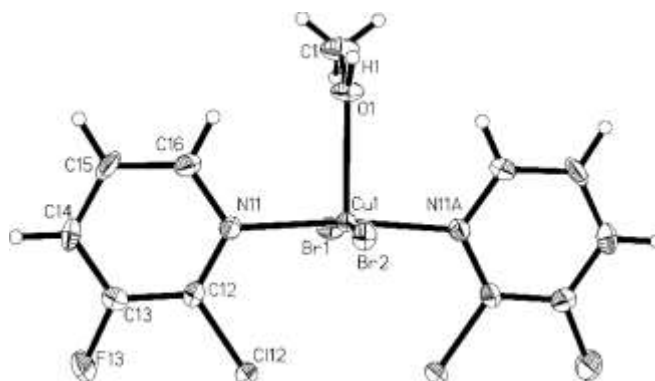


**Figure 8:** A plot of the molecular unit of compound **1** showing 50% probability thermal ellipsoids. The asymmetric unit, copper coordination sphere and hydrogen atom whose position was refined are labeled.

### Magnetic properties

Magnetization data for **1-4** were collected as a function of field and temperature on powdered samples which had been confirmed by powder X-ray diffraction to be the same phase as the single crystal structures with no detectable impurities. In all cases, plots of  $M(H)$  were linear to at least 5 kOe and no hysteresis was observed. The magnetization was near saturation for all compound at 50 kOe with a value near 6,000 emu/mol in agreement with a  $S = \frac{1}{2}$  ion with  $g \sim 2.1$ . No maxima were observed in  $\chi(T)$  for any of the compounds. Data are shown in Figures 9-12 and the results of the various fits to the data are collected in Table 6.

Data for **1** (Figure 9) show a virtual absence of interactions except at the very lowest temperatures where there is evidence that very weak ferromagnetic exchange may be occurring. A Curie-Weiss fit of the data gave a positive, but very small, value of  $\theta$  (0.21(9) K).

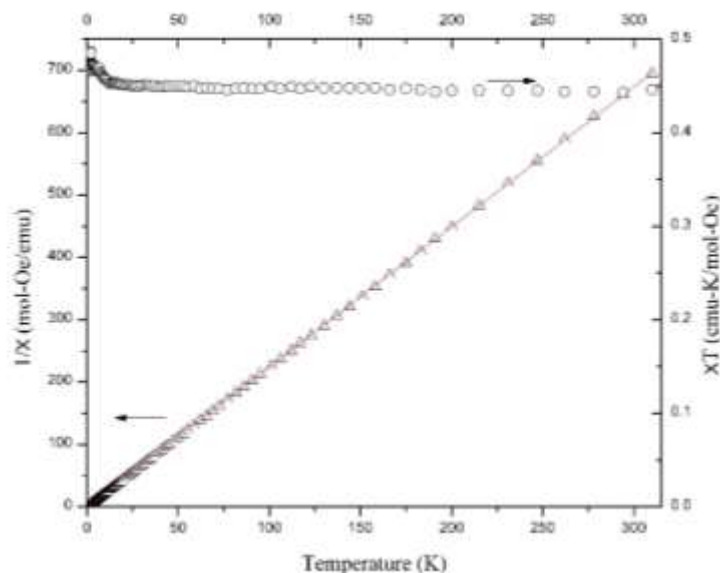


**Figure 9:**  $\chi T(T)$  ( $\circ$ ) and  $1/\chi(T)$  ( $\Delta$ ) for **1**. The solid line shows a fit of  $1/\chi$  vs.  $T$  to the Curie-Weiss law.

Compound **2** exhibits clear ferromagnetic interactions (Figure 10). Based upon the crystal structure analysis, the  $\chi T(T)$  data were fit to the 1D-ferromagnetic chain model<sup>46</sup> which gave an exchange constant of 1.72(2) K. This was corroborated by a fit of the Curie-Weiss plot which resulted in  $\theta = 0.62(4)$  K.

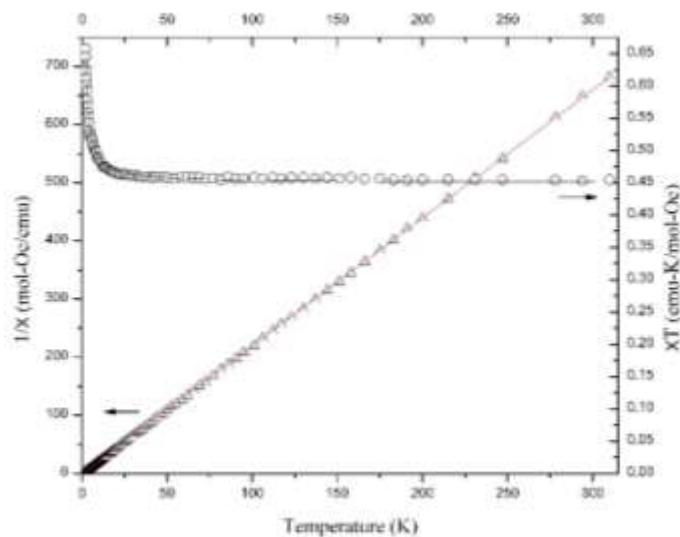


**Figure 10:**  $\chi T(T)$  ( $\circ$ ) and  $1/\chi(T)$  ( $\Delta$ ) for **2**. The solid lines show fits of  $\chi T(T)$  to the 1D-ferromagnetic chain model and of  $1/\chi(T)$  to the Curie-Weiss law.

In contrast to **2**, magnetic data for **3** showed weak antiferromagnetic interactions. The data were fit to the 1D-antiferromagnetic chain model<sup>46</sup> which resulted in  $J/k_B = -1.21(1)$  K, in good agreement with the fit of  $1/\chi$  to the Curie-Weiss law which gave  $\theta = -0.55(6)$ .

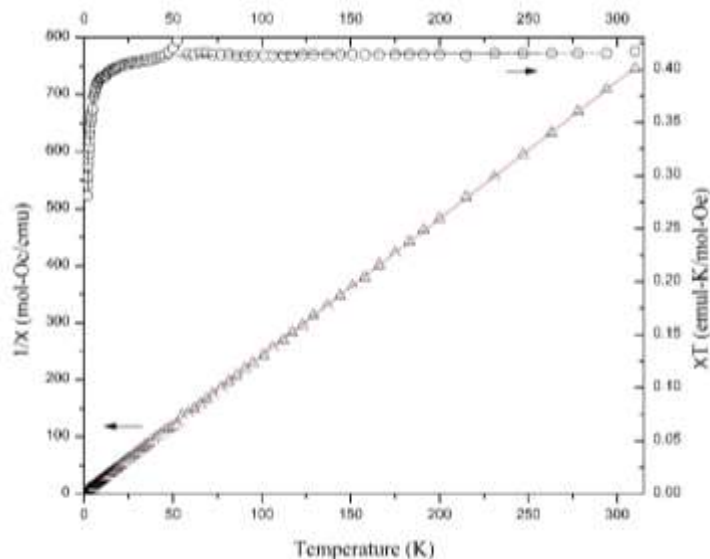


**Figure 11:**  $\chi T(T)$  ( $\circ$ ) and  $1/\chi(T)$  ( $\Delta$ ) for **3**. The solid lines show fits of  $\chi T(T)$  to the 1D-antiferromagnetic chain model and of  $1/\chi(T)$  to the Curie-Weiss law.

Compound **4** greatly resembles the behavior of **1** except that the possibility of very weak ferromagnetic interactions has been replaced by the possibility of very weak antiferromagnetic interactions.  $\chi T(T)$  is flat except at the lowest temperatures where a slight downturn is observed. Fitting the  $1/\chi(T)$  data to the Curie-Weiss law gave  $\theta = 0.02(14)$ , zero within experimental error.

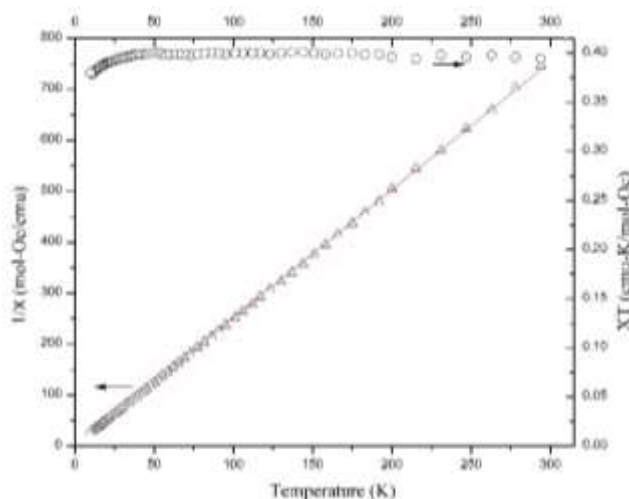


**Figure 12:**  $\chi T(T)$  ( $\circ$ ) and  $1/\chi(T)$  ( $\Delta$ ) for **4**. The solid line shows a fit of  $1/\chi$  vs.  $T$  to the Curie-Weiss law.

**Table 6:** Fitting Results for Magnetic data of compounds 1-4.

Compound	Model	CC(emu-K/mol-Oe)	$J/k_B$ (K)	$\theta$ (K)
<b>1</b>	Curie-Weiss	0.445(2)		0.21(9)
<b>2</b>	FM 1D chain	0.450(1)	1.72(2)	
	Curie-Weiss	0.454(1)		0.62(4)
<b>3</b>	AFM 1D chain	0.417(1)	-1.20(1)	
	Curie-Weiss	0.416(1)		-0.55(6)
<b>4</b>	Curie-Weiss	0.398(1)		0.02(14)

## DISCUSSION

Although a very wide variety of bis(subpy)CuX<sub>2</sub> compounds (subpy = pyridine or substituted pyridine) have been presented in the literature,<sup>12,15,18,19,20,47</sup> only two crystal structures of 2,3-dihalopyridine compounds have been reported, 2,3-dichloropyridine<sup>48</sup> and 3-bromo-2-iodopyridine;<sup>49</sup> no transition metal complexes of 2,3-dihalopyridines have been reported. Thus, **1-4** provide information on a new group of copper halide-pyridine complexes. Compounds **1** and **2** are both five-coordinate with two 2-Cl-3-Fpy ligands, two chloride ions and a coordinated solvent molecule. Attempts to prepare the solvent free molecule, both directly and by desolvation of either **1** or **2** were unsuccessful. The high volatility of the ligand (it is a liquid at room temperature) presumably contributes to its partial loss during attempts to desolvate the complexes. There is precedent for the coordination of a solvent molecule, especially an O-coordinated species, to (subpy)<sub>2</sub>CuX<sub>2</sub> structures with chelating subpy species (bipyridine or phenazine complexes),<sup>50</sup> but such complexes with independent pyridine-based ligands are much less common.<sup>21,42,51</sup> All of the non-chelating systems show near square pyramidal geometry in a trans configuration with the solvent molecule in the axial site as observed in **1**, **2** and **4**. The syn conformation of the pyridine ligands **1**, **2** and **4** is primarily responsible for limiting the complexes to 5-coordinate; the potential coordination site trans to the solvent molecule is sterically blocked by the 2-substituents on the pyridine rings.

Halogen bonding is observed in **1-4** as well and is responsible for the formation of chain structures within the lattice parallel to the *c*-axis. The most significant halogen bonds are of the C-X'...X-M halogen/halide type (X' = halogen, X = halide, M = metal ion)<sup>52</sup> where the C-X'...X angle is near 180° and the X'...X-M angle is near 90° (see Table 4). In all cases the X'...X distances are less than the sum of the van der Waals radii (Cl = 1.75 Å, Br = 1.87 Å).<sup>53</sup> The Cl...Cl distances for **1** and **2** range from 3.290-3.376 Å while the corresponding Cl...Br distances in **3** and **4** are 3.442 Å and 3.477 Å, slightly longer as expected due to the larger Br radius. Further, because the X groups are anions, they are expected to have even larger effective radii, making the observed contacts even more significant. No significant halogen bonding was observed to the fluorine substituent in any of the complexes.

The effects of hydrogen bonding are distinctly different for **1** and **4** compared to both **2** and **3** (Table 3). In the methanol solvate complexes, there is a hydrogen bond between the methanol O-H group and a halide ion on an adjacent molecule which further stabilizes the chains generated parallel to the *c*-axis by the halogen bonding (Figure 2a). In compound **2**, however, there is an additional hydrogen bond as a result of the substitution of water for methanol (Figure 5). The O1-H1B...Cl1 hydrogen bond provides a separate connection, one that is independent of the halogen bonding between molecules in the original chain structures. Further, the two hydrogen bonds in **2** have very different temperatures



dependencies as shown by comparison of data from **2** (150 K) and **2RT** (293 K). The O1-H1A...Cl2 hydrogen bond (linking the same molecules as the halogen bonds) changes only very slightly upon cooling [ $d_{O\dots Cl2} = 3.213$  (RT) vs. 3.186 (low T)], but a more substantial decrease is observed for the O1-H1B...ClA linkage [ $d_{O\dots Cl1} = 3.700$  Å (RT) vs. 3.572 Å (low T)] over the same temperature range. We presume that the difference is, in part, a result of the halogen bonding which may limit the closest approach of molecules parallel to the *c*-axis (the X'...X distances decreases by 0.036 Å over the same temperature range). The weaker interactions/greater initial spacing between the chains allows for a greater thermal contraction parallel to the *a*-axis upon cooling. There are no traditional hydrogen bond donors in **3**.

Analysis of the magnetic data shows three distinct results. Compounds **1** and **4** show virtually no exchange (the possible exchange in both cases is weak enough to be within experimental error of zero). Their equivalent behavior is logical given that the two compounds are isomorphous. However, the absence of measurable magnetic exchange in the compounds, more importantly, shows that neither the hydrogen bonding, nor the halogen bonding, that links the molecules into the chain structure parallel to the *c*-axis provides an effective superexchange pathway.

This leaves the ferromagnetic and antiferromagnetic exchange observed in **2** and **3** respectively. Qualitative parameters for the two-halide superexchange pathway have been established for bromide complexes<sup>54</sup> which shows that the exchange is maximized as  $d_{x\dots x}$  decreases,  $\theta$  approaches 180° and the torsion angle ( $T$ ) approaches 0° or 180° (see Table 5 for definition of terms). Antiferromagnetic exchange has been observed in chloride complexes at distances much greater than that observed for **2**,<sup>33,34</sup> but the  $\theta$  angles involved are much closer to 90° than the optimal 180°. Further, one would expect antiferromagnetic exchange via the two-halide pathway, and weak ferromagnetic exchange is observed. The 'extra' hydrogen bond observed in the complex may provide an explanation. Weak ferromagnetic exchange, propagated by hydrogen bonding, has been reported in the literature.<sup>55</sup> The magnitude of the interaction corresponds well with those previous reports. The distinct shortening of the D...A distance in that hydrogen bond upon cooling also supports the possibility that this is, indeed, the appropriate superexchange pathway. Finally, the antiferromagnetic exchange observed in **3** is typical for such complexes. The two-halide parameters are far from ideal,<sup>54</sup> in agreement with the weak exchange observed, but antiferromagnetic exchange in such compounds has been seen at Br...Br distances up to 5.0 Å.<sup>33</sup>

## Conclusions

In this study the synthesis as well as spectroscopic, structural and magnetic properties of four copper halide-pyridine complexes is reported. Of these structures two are coordinated to a molecule of

methanol (**1** and **4**), one is coordinated to a molecule of water (**2**) and compound **3** is desolvated. Compounds **1-4** demonstrate lattice stabilizing halogen bonding and compounds **1**, **2** and **4** also showing lattice stabilizing hydrogen bonding. Neither the halogen nor hydrogen bonding in **1** and **4** provide an effective superexchange pathway thus the compounds demonstrate negligible magnetic exchange. The additional hydrogen bonding in compound **2** contributes toward its magnetic behavior, likely propagating the observed weak ferromagnetic exchange as has been reported previously.<sup>55</sup> Compound **3** demonstrates typical antiferromagnetic exchange via the two-halide superexchange pathway in agreement with comparable reports in the literature.

To our knowledge, these are the first published structures of 2,3-dihalopyridine copper complexes; it is curious why complexes of this type have not been previously synthesized and reported. The difficulty and current failure to synthesize bis(2-chloro-3-fluoropyridine)dichloridocopper(II) without a coordinated solvent molecule, while synthesis of both methanol and water coordinated complexes are facile may speak to the question. Clearly, the halogen substituents would reduce the electron density in the pyridine ring making it a poorer ligand. The synthesis of the solvated complexes suggests that the resulting reduced electron density at the Cu(II) ion makes it more electrophilic and hence more susceptible to attack by nucleophilic solvents. The balance in electron density is clearly quite fine as substitution of the less electronegative bromide ion for chloride ion on the Cu(II) allowed isolation of the non-solvated molecule. Additional work is in progress to expand the family of compounds and examine the relationship between the 4- and 5-coordinated complexes further. Synthesis and characterization of similar 2,3-dihalopyridine complexes are in progress and appear promising and work to synthesize the parent bis(2-chloro-3-fluoropyridine)dichloridocopper(II) continues.

#### **Acknowledgements:**

The authors are grateful to PCISynthesis, Inc. for funds toward the purchase of the X-ray powder diffractometer, the National Science Foundation (IMR-0314773) toward the purchase of the MPMS SQUID magnetometer and the Kresge Foundation toward the purchase of both.

## References

---

1. G.B. Kauffman, S. Padhye. *Coord. Chem. Rev.*, **63**, 127 (1985).
2. I. Murase, G. Vuckovic, M. Kodera, H. Hirotaka, N. Matsumoto, S. Kida. *Inorg. Chem.*, **30**, 728 (1991).
3. O.M. Yaghi, H. Li, T.L. Groy. *J. Am. Chem. Soc.*, **118**, 9096 (1996).
4. A.L. Garay, A. Pichon, S.L. James. *Chem.Soc.Rev.*, **36**, 846 (2007).
5. R. Ruiz, M. Julve, J. Faus, F. Lloret, M. C. Muñoz, Y. Journaux, C. Bois. *Inorg. Chem.*, **36**, 3434 (1997).
6. J.P. Costes, J.M. Clemente-Juan, F. Dahan, J. Milon. *Inorg. Chem.*, **43**, 8200 (2004).
7. C.P. Landee, M.M. Turnbull, *Eur. J. Inorg. Chem.*, 2266 (2013).
8. R. Peng, D. Li, T. Wu, X.-P. Zhou, S.W. Ng *Inorg. Chem.*, **45**, 4035 (2006).
9. Y. Lei, D.R. Powell, R.P. Houser. *Dalton Trans.*, **9**, 955 (2007).
10. B. Kozlevcar, P. Segedin. *Croat. Chem. Acta.*, **81**, 369 (2008).
11. M. Kato, H.B. Jonassen, J.C. Fanning. *Chem. Rev.*, **64**, 99 (1964).
12. M. Matsuura. *Phys. Lett. A*, **34**, 274 (1971).
13. M. Thede, F. Xiao, Ch. Baines, C. Landee, E. Morenzoni, A. Zheludev. *Phys. Rev. B.*, **86**, 180407 (2012).
14. M. Barquin, M.J. Garmendia, L. Larrinaga, E. Pinilli, M.R. Torres. *Inorg. Chim. Acta*, **362**, 2334 (2009).
15. R.A. Ahmadi, F. Hasanvand, G. Bruno, H.A. Rudbari, S.Amani. *Inorg. Chem.*, **42**, 6713 (2013).
16. D.P. Graddon, R. Schulz, E.C. Watton, D.G. Weeden, *Nature*, **198**, 1299 (1963).
17. R.N. Patel, D.V. R.Rao, *Ind. J. Chem.*, **6**, 112 (1968).
18. P. Singh, D.Y. Jeter, W.E. Hatfield, D.J. Hodgson. *Inorg. Chem.*, **11**, 1657 (1972).
19. J.A.C. Van Ooijen, J. Reedijk. *Inorg. Chim. Acta*, **25**, 131 (1977).
20. V.H. Crawford, W.E. Hatfield, *Inorg. Chem.*, **16**, 1336 (1977).
21. W.E. Marsh, W.E. Hatfield, D.J. Hodgson. *Inorg. Chem.*, **21**, 2679 (1982).
22. A. Aguirrechú-Comeron, J. Pasan, J. Gonzalez-Platas, J. Ferrando-Soria, R. Hernandez-Molina, R. *J. Struct. Chem.*, **56**, 1563 (2015).
23. W. Zhang, J.R. Jeitler, M.M. Turnbull, C.P. Landee, M. Wei, R.D. Willett, *Inorg. Chim. Acta*, **256**, 183 (1997).
24. R.L. Forman, A.J. Gale, C.P. Landee, M.M. Turnbull, J.L. Wikaira, *Polyhedron*, **89**, 76 (2015).
25. R.L. Forman, C.P. Landee, J.L. Wikaira, M.M. Turnbull, *Eur. Chem. Bull.*, **3**, 190 (2014).
26. B.L. Solomon, C.P. Landee, M.M. Turnbull, J.L. Wikaira. *J. Coord. Chem.*, **67**, 3953 (2014).
27. C.A. Krasinski, B.L. Solomon, F.F. Awwadi, C.P. Landee, M.M. Turnbull, J.L. Wikaira, *J. Coord. Chem.*, **70**, 914 (2017).
28. M. Abdalrahman, C.P. Landee, S.G. Telfer, M.M. Turnbull, J.L. Wikaira, *Inorg. Chim. Acta*, **389**, 66 (2012).
29. S.N. Herringer, M.M. Turnbull, C.P. Landee, J.L. Wikaira, *Dalton Trans.*, **40**, 4242 (2011).
30. S.N. Herringer, M. Deumal, J. Ribas-Ariño, J.J. Novoa, C.P. Landee, J.L. Wikaira, M.M. Turnbull. *Chem.-Eur. J.*, **20**, 8355 (2014).
31. S.N. Herringer, C.P. Landee, M.M. Turnbull, J. Ribas-Ariño, J.J. Novoa, M. Polson, J.L. Wikaira, *Inorg. Chem.*, **56**, 5441 (2017).
32. F.M. Woodward, C.P. Landee, J. Giantsidis, M.M. Turnbull, C. Richardson. *Inorg. Chim. Acta*, **324**, 324 (2001).
33. F.M. Woodward, A.S. Albrecht, C.M. Wynn, C.P. Landee, M.M. Turnbull. *Phys. Rev. B.*, **65**, 144412 (2002).

- 
34. C.P. Landee, M.M. Turnbull, C. Galeriu, J. Giantsidis, F.M. Woodward, *Phys. Rev. B, Rapid Commun.*, **63**, 100402R (2001).
35. A. Shapiro, C.P. Landee, M.M. Turnbull, J. Jornet, M. Deumal, J.J. Novoa, M. Robb, W. Lewis. *J. Am. Chem. Soc.*, **129**, 952 (2007).
36. R. L. Carlin. *Magnetochemistry*; Springer-Verlag: Berlin, 1986.
37. SAINT. Ver. 8.34A. (Bruker-AXS, 2014).
38. G. Sheldrick, SADABS, *University of Göttingen, Germany*, 1996.
39. G.M. Sheldrick *Acta Cryst. A*, **64**, 112 (2008).
40. G.M. Sheldrick *Acta Cryst. C*, **C71**, 3 (2015).
41. A.W. Addison, T.N. Rao, J. Reedijk, J. van Rijn, G.C. Verschoor. *J. Chem. Soc., Dalton Trans.*, 1349 (1984).
42. Z.-M. Jin, Z.-G. Li, B. Tu, Z.-L. Shen, M.-L. Hu. *Acta. Cryst. E*, **61**, 2566 (2005).
43. a) G.A. van Albada, S. Tanase, I. Mutikainen, U. Turpeinen, J. Reedijk. *Inorg. Chim. Acta*, **361**, 1463 (2008). b) K.C. Shortsleeves, L.N. Dawe, C.P. Landee, M.M. Turnbull. *Inorg. Chim. Acta*, **362**, 1859 (2009).
44. a) O.V. Koval'chukova, V.E. Zavodnik, A.F. Shestakov, S.B. Strashnova, B.E. Zaitsev. *Russ. J. Inorg. Chem.*, **55**, 230 (2010). b) Wen-Bo Shi, Ai-Li Cui, Hui-Zhong Kou *Cryst.Growth Des.*, **12**, 3436 (2012).
45. B. Li, S.Q. Zang, L.Y. Wang, T.C.W. Mak, *Coord. Chem. Rev.*, **308**, 1 (2016).
46. C.P. Landee, M.M. Turnbull, *J. Coord. Chem.*, **67**, 375 (2014).
47. The references provided constitute a very small sample of the published papers.
48. L.J. Luo, J.-Q. Weng *Acta Cryst. E*, **67**, o2211(2011).
49. J.S. Dhaua, A. Singh, Y. Kasetti, S. Bhatia, P.V. Bharatam, P. Brandao, V. Felix, K.N. Singh *Tetrahedron*, **69**, 10284 (2013).
50. a) J. Emsley, M. Arif, P.A. Bates, M.B. Hursthouse *J. Chem. Soc.,Dalton Trans.*, 2397 (1987). b) J. Emsley, M. Arif, P.A. Bates, M.B. Hursthouse *J. Crystallogr. Spectrosc. Res.*, **17**, 605 (1987). c) H.S. Preston, C.H.L. Kennard *J. Chem. Soc. A*, 2955 (1969). d) K. Oyaizu, M. Ueno, H. Li, E. Tsuchida *Bull. Chem. Soc. Jpn.*, **74**, 869 (2001). e) R.D. Willett, G. Pon, C. Nagy *Inorg. Chem.*, **40**, 4342 (2001). f) A. Giordana, E. Priola, E. Bonometti, P. Benzi, L. Operti, E. Diana. *Polyhedron*, **138**, 239 (2017).
51. a) D.R. Turner, B. Smith, A.E. Goeta, I.R. Evans, D.A. Tocher, J.A.K. Howard, J.W. Steed *CrystEngComm*, **6**, 633 (2004). b) S. Banerjee, P. Dastidar *CrystEngComm*, **15**, 9415 (2013).
52. a) L. Brammer. *Chem. Soc. Rev.*, **33**, 476 (2004). b) L. Brammer, G. Espallargas, S. Libri. *CrystEngComm* (2008), **10**, 1712. c) H.R. Khavasi, A. Azhdari Tehrani. *Inorg. Chem.*, **52**, 2891 (2013). d) F.F. Awwadi, D. Taher, S.F. Haddad, M.M. Turnbull. *Cryst. Growth Des.*, **14**, 1961 (2014). e) R.D. Willett, F.F. Awwadi, R.T. Butcher, S.F. Haddad, B. Twamley, *Cryst. Growth Des.*, **3**, 301 (2003).
53. A. Bondi. *J. Phys. Chem.*, 68, 441 (1964).
54. M.M. Turnbull, C.P. Landee, B.M. Wells. *Coord. Chem. Rev.*, **249**, 2567 (2005).
55. a) E. Hernandez, M. Mas, E. Molins, C. Rovira, J. Veciana. *Angew. Chem., Int. Ed. Engl.*, **32**, 882 (1993). b) J. Cirujeda, E. Hernandez-Gasio, C. Rovira, J.-L. Stanger, P. Turek, J. Veciana. *J. Mat. Chem.*, **5**, 243 (1995). c) J. Cirujeda, M. Mas, E. Molins, F. Lanfranc de Panthou, J. Laugier, J.G. Park, C. Paulsen, P. Rey, C. Rovira, J. Veciana. *J. Chem. Soc., Chem. Commun.*, 709 (1995).